OBSERVATIONS OF NEARSHORE AND SURF ZONE WIND STRESS

Behnam Shabani[1], Peter Nielsen[1] and Tom Baldock[1]

Field data of the wind stress over surf zone waves is presented from an open ocean beach on the East Australian Coast. Two ultrasonic anemometers were deployed at nominal heights of 5 and 10 m above the water surface in the intertidal and inner surf zones, with concurrent measurements of water levels and offshore wave parameters. Considering near-neutral conditions only, the wind drag coefficients were found to systematically change with the wind angle of approach relative to the shoreline, and are much smaller for longshore wind than during onshore wind. The concept of an apparent wave steepness changing with wind direction is suggested to explain this behaviour. The drag coefficients over the surf zone during onshore wind and near-neutral conditions were determined to be almost twice the values expected at the same wind speed and open ocean conditions. The observed Charnock coefficient was similarly an order of magnitude larger than open ocean values. A wave celerity of the order of that expected in the inner surf zone is required to explain the observed large roughness and drag coefficients using existing wave-age dependent parameterisations. This suggests that the slower wave celerity in the surf zone is an important contributor to the increased wind stress, in addition to the sawtooth wave shape.

Keywords: air-sea interaction; wind stress; drag coefficient; surf zone; nearshore region; field study; storm surge

INTRODUCTION

Storm surges are identified as a major hazard for coastal low-lying areas. Recent examples include Tropical Cyclone Yasi (QLD, 2011) and Hurricane Ike (Texas, 2008), which both generated 5 m storm surges and significant damage. Wind stress on the ocean surface plays an important role in generating storm surges. Predicting the wind shear stress and drag coefficient over the ocean is therefore critical for storm surge modelling. Since the wind setup is inversely proportional to the water depth, the wind stress and the wind drag coefficient over the nearshore region and the surf zone is needed for accurate modelling. However, limited data exists from these regions, and offshore wind drag coefficients are often used to model storm surges (e.g. Lentz et al., 1999; Reniers et al., 2004). Experimental and field data are therefore essential to identify potential differences between the wind drag coefficient over deep ocean and that over the surf zone in order to improve modelling results.

The wind shear stress (τ) is typically expressed in terms of the wind drag coefficient (C_D) or alternatively the aerodynamic roughness ($z_\circ$). Over the past sixty years, following the pioneering work of Charnock (1955), numerous studies focused on quantifying these parameters over the ocean and formulating them as a function of wind and wave characteristics. Over the deep ocean, it has been proposed that the drag coefficient (C_D) increases with increasing mean wind velocity ($\bar{u}$), and a linear parameterisation ($C_D = a\bar{u} + b$) is often suggested to express this behaviour (Garratt, 1977; Geernaert et al., 1987; Smith et al., 1992; Yelland and Taylor, 1996; Vickers and Mahrt, 1997; Drennan et al., 1999). A similar but non-linear relationship is also implicit within the Charnock (1955) parameterisation of the ocean surface roughness, $z_\circ = \alpha {u_*}^2/g$, in which u_* is the friction velocity and g is the gravitational acceleration. Smith (1980), Wu (1980), Geernaert et al. (1986) and Johnson et al. (1998), among others, adopted the Charnock-type parameterisation and proposed experimental values of the Charnock coefficient (α). However, it is not possible to envision a general drag law solely based on the wind speed as the state of the ocean surface is also controlled by the wind fetch, wind duration, and water depth. Wave-aware drag parameterisations were therefore proposed in response to the observed variabilities among different wind speed dependent parameterisations (Kitaigorodskii and Volkov, 1965). For this purpose, it has been suggested to parameterise the Charnock coefficient as a function of the wave age, $\alpha = a(c_p/u_*)^{-b}$, where c_p is the peak wave celerity and c_p/u_* is the wave age (Maat et al., 1991; Smith et al., 1992; Vickers and Mahrt, 1997; Johnson et al., 1998; Oost et al., 2002; Drennan et al., 2003). Other alternatives include Taylor and Yelland (2001) parameterisation of the roughness based on the wave steepness, $z_\circ/H_s = a(H_s/\lambda_p)^b$, and Hwang (2004) wave length scaling of the roughness, $z_\circ/\lambda_p = a(\omega_p u_*/g)^b$, where H_s, λ_p and ω_p are respectively the significant wave height, peak wave length and peak angular wave frequency. A detailed review of existing studies of wind stress on the ocean surface has recently been provided in Shabani et al. (2014), while a comprehensive discussion of the air-sea interaction topic and associated physical processes is given in Shabani (2013).

Given the interest in the problem of wind-wave generation, over the past sixty years, studies of the wind stress on the ocean primarily focused on deep water. The need for wave-aware drag parameterisations further led to an interest in shallower regions of the ocean. The objective was to widen the range of measured wave age values and develop more reliable wave-age dependent drag parameterisations in order to gain a better understanding of the early stages of wave development. With this objective, the

[1]School of Civil Engineering, University of Queensland, Australia

regions with strong wave shoaling and breaking were often avoided to prevent *contamination* of data. As such, the wind stress over coastal water and in particular the surf zone has remained largely unexplored, despite its importance for modelling storm surges and nearshore currents. Recently, Zachry et al. (2009) collected wind stress data using the Turbulent Intensity (TI) method in a coastal area during Hurricane Ike. Measured drag coefficients increased very slowly with the wind speed, in comparison with the open ocean data. At high wind speed, the data were quite similar to open ocean drag coefficients, but at low and moderate speeds, they were much larger than deep water values. However, there were uncertainties due to potential *Internal Boundary Layer* (IBL) effects arising from the exposure of the land between the waterline and the measurement point, during low and moderate wind speed, especially given the low measurement height of only about 2 m above the ground and the long 90 m land fetch at full waterline recession. At high wind speed during the peak of the event, nevertheless, the measurement point was drowned, thus avoiding potential contamination by IBL effects. Similarly, Shabani et al. (2011) presented wind drag coefficient and roughness data collected from two coastal sites using the wind profile method, and concluded that the wind stress is enhanced in the nearshore region. However, potential IBL effects were not analysed, leading to similar uncertainties as in Zachry et al. (2009). On the other hand, Vickers and Mahrt (2010) recently suggested that the aerodynamic roughness in the coastal zone is smaller than those given by widely-used open-ocean models during weak and moderate winds. Roughness values in the coastal zone, however, were similar to the open ocean values during high wind speeds. It should be mentioned though that the datasets used in Vickers and Mahrt (2010) were aircraft observations over shallow water and not the surf zone.

As the review above indicates, the wind stress on the surf zone has remained largely unexplored, and differences are expected since waves in the surf zone and surrounding coastal water travel with much slower speeds than deep water waves. At the same time, surf zone waves exhibit different shapes from the waves in other regions of the ocean. To address this issue, a field campaign was conducted to investigate the wind shear stress on the surf zone and surrounding coastal water. This paper presents the results of the field experiment, which adopted the eddy correlation technique – otherwise known as the direct method to obtain the shear stress. The experiment avoids previous uncertainties by deploying instruments very close to the waterline, and filtering out any internal boundary layer effects through appropriate quality controls.

THEORETICAL BACKGROUND

The Reynolds shear stress (τ), or the turbulent flux of momentum, at a given elevation above the ocean surface is defined as:

$$\tau = -\rho\overline{u'w'} \tag{1}$$

where ρ is the air density; u and w are respectively horizontal and vertical components of instantaneous wind velocity at that elevation; the prime symbol denotes turbulent fluctuations of a quantity relative to its mean value – e.g. $u' = u - \bar{u}$; and the overbar indicates time-averaging over a suitable period. Following the assumption of a constant shear stress layer, one may consider τ at its measurement height to have the same value as the shear stress at the boundary surface ($\tau_\circ$). The surface flux of momentum is often expressed in the form of a wind shear velocity (u_*) as:

$$\tau_\circ = \rho {u_*}^2 \tag{2}$$

The shear velocity is a scaling parameter for the vertical gradient of the mean wind speed, based on Monin-Obukhov similarity theory:

$$\frac{\partial \bar{u}}{\partial z} = \frac{u_*}{\kappa z}\phi_m(\frac{z}{L}) \tag{3}$$

in which z is the elevation measured positive upward from the boundary surface, and κ is the von-Karman constant. The non-dimensional velocity gradient function ϕ_m is a function of the stability parameter (z/L), where L is the Monin-Obukhov length scale defined as:

$$L = -\frac{{u_*}^3\bar{\theta}_v}{g\kappa\overline{\theta_v' w'}} \tag{4}$$

where θ_v is the virtual temperature of air. Integrating Equation (3) from the roughness height $z_\circ$ to the elevation z gives the vertical distribution of the mean wind speed:

$$\bar{u} = \frac{u_*}{\kappa}\left[\ln\frac{z}{z_\circ} - \psi_m(\frac{z}{L})\right] \tag{5}$$

in which ψ_m is the stability function, and is the integrated form of the gradient function (ϕ_m).

Under neutral atmospheric stability conditions, Equation (5) reduces to the well-known logarithmic wind velocity profile:

$$\bar{u} = \frac{u_*}{\kappa} \ln \frac{z}{z_\circ} \tag{6}$$

The non-dimensional velocity gradient (ϕ_m) and the stability function (ψ_m) alter the velocity profile from the logarithmic distribution according the local stability condition described by the stability parameter (z/L). Following Businger et al. (1971), the gradient function is expresses as:

$$\phi_m(\frac{z}{L}) = \left(1 - \alpha_b \frac{z}{L}\right)^{-\frac{1}{4}} \quad \text{when } \frac{z}{L} < 0 \tag{7}$$

$$\phi_m(\frac{z}{L}) = 1 + \beta_b \frac{z}{L} \quad \text{when } \frac{z}{L} > 0 \tag{8}$$

with numerical coefficients being $\alpha_b = 20$, $\beta_b = 5$ and $\kappa = 0.4$, as in Yelland and Taylor (1996). Following Paulson (1970), the stability function (ψ_m) is expressed as:

$$\psi_m(\frac{z}{L}) = 2\ln\left(\frac{1+{\phi_m}^{-1}}{2}\right) + \ln\left(\frac{1+{\phi_m}^{-2}}{2}\right) - 2\tan^{-1}\left({\phi_m}^{-1}\right) + \frac{\pi}{2} \quad \text{when } \frac{z}{L} \le 0 \tag{9}$$

$$\psi_m(\frac{z}{L}) = 1 - \phi_m \quad \text{when} \frac{z}{L} \ge 0 \tag{10}$$

The wind shear stress is often expressed in terms of a wind drag coefficient (C_{Dz}) through the conventional relationships:

$$C_{Dz} = \frac{\tau_\circ}{\rho_a \bar{u}_z^2} = \left(\frac{u_*}{\bar{u}_z}\right)^2 \tag{11}$$

where $\bar{u}_z$ is the mean wind speed at height z above the sea surface. Typically, $\bar{u}_{10}$ is used for this purpose.

The vertical profile of the wind velocity is dependent on the local stability conditions as described by Eqs. (3) and (5). The effect of the stability on the drag coefficient is represented by the stability-dependent $\bar{u}_z$ in Eq. (11). In order to compare the drag coefficients measured under different stability conditions with each other, the stability effects should be accounted for to report the equivalent drag coefficient under neutral stability conditions. The neutral-equivalent drag coefficient (C_{DNz}) is simply defined based on the mean wind speed under the neutral stability conditions ($\bar{u}_{Nz}$) as:

$$C_{DNz} = \frac{\tau_\circ}{\rho_a \bar{u}_{Nz}^2} \tag{12}$$

The neutral wind speed ($\bar{u}_{Nz}$) is obtained from Eq. (6). Using the general form of the wind velocity profile in Eq. (5) and that under neutral stability conditions in Eq. (6), C_{DNz} and C_{Dz} are related to each other as:

$$C_{DNz} = \left[{C_{Dz}}^{-\frac{1}{2}} + \frac{\psi_m\left(\frac{z}{L}\right)}{\kappa}\right]^{-2} \tag{13}$$

The wind measurements may not necessarily be taken at the 10 m elevation. However, it is customary to report the drag coefficient with reference to the 10 m wind velocity in order to make various measurements comparable with one another. For this purpose, the wind velocity profile in Eq. (6) can be used to express the wind velocities at any two elevations such as z_1 and z_2 in terms of each other, with z_2 taken as 10 m for the present study. Similarly, the drag coefficients that are referenced to the wind velocity at these two elevations can also be correlated with each other:

$$\frac{C_{DNz_2}}{C_{DNz_1}} = \left(\frac{\bar{u}_{Nz_1}}{\bar{u}_{Nz_2}}\right)^2 = \left(\frac{\ln \frac{z_1}{z_\circ}}{\ln \frac{z_2}{z_\circ}}\right)^2 \tag{14}$$

FIELD EXPERIMENT

A month-long intensive field experiment, namely the North Stradbroke 2012 field campaign, was conducted from May 4th to June 1st, 2012 to obtain wind shear stress measurements over the surf zone. The experiment was carried out from an open ocean beach near Point Lookout, North Stradbroke Island, Australia (Figure 1). The eastern beach is open to South Pacific Ocean via the Coral Sea and has a bearing of 210°, and is aligned favourably normal to the dominant South-Easterly winds. Measurements over the course of the experiment were mostly continuous, and were interrupted only for about an hour on each day for instrument maintenance and data retrieval.

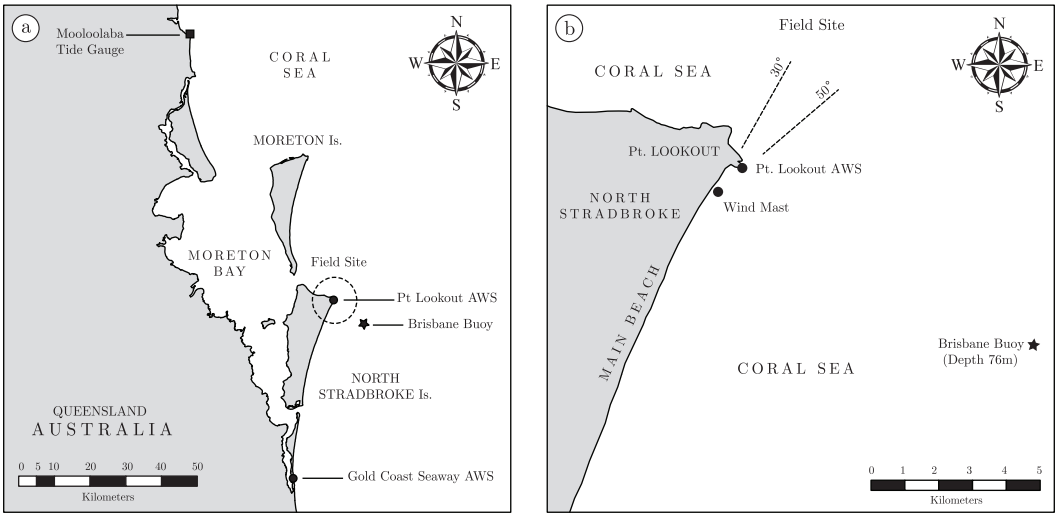

Figure 1: Field site of the North Stradbroke 2012 campaign: (*a*) the site locality, and (*b*) a close-up view of the site. The beach is oriented along 30° – 210° direction. Wind directions in the range of 30° – 50° are obscured by the cliffs at Point Lookout. The location of third-party tide, wave, and weather monitoring stations are also marked on the figure.

Wind Stress Measurement Technique

Several methods are available for measuring the wind shear stress on the ocean surface, such as the eddy correlation technique, profile method, inertial dissipation technique, etc. Among them, the eddy correlation technique, otherwise known as the direct method, has been the most widely used wind stress measurement technique, and has become the standard method in recent years. When combined with a careful quality control and necessary corrections, the eddy correlation technique provides a robust and reliable approach, and was therefore used during the North Stradbroke 2012 field experiment.

In the eddy correlation method, fluctuating components of horizontal and vertical wind velocities (u' and w') are measured using a fast response anemometer at a given elevation in order to evaluate the wind shear stress directly from $\tau = \rho\overline{u'w'}$ – i.e. Equation (1). Two *Gill Wind Master Pro* ultrasonic anemometers with a sampling rate of 32 Hz were used for this purpose during the 2012 experiment. The anemometers were mounted at nominal heights of 5 and 10 m above the ground on a 10 m high wind mast which was deployed in the intertidal zone at the landward edge of the surf zone. The mast was often located within the water during high tide. The proximity of the wind mast to the shoreline ensured that the anemometers at 5 and 10 m heights were not influenced by the potential internal boundary layer effects of the exposed beach between the mast and the shoreline. At the same time, quality controls were also implemented to filter out a limited number of data blocks collected during very low tide conditions in order to avoid such internal boundary layer effects, and to ensure that the assumption of constant stress layer is not violated. Full details of the experiment, instrumentation, and quality controls are discussed in Shabani (2013) and Shabani et al. (2014).

Once the shear stress is known, the shear velocity (u_*) and the drag coefficient (C_{Dz}) are evaluated from Eq. (2). The drag coefficient is subsequently converted to the equivalent drag coefficient under neutral stability conditions. For this purpose, the buoyancy flux $\overline{\theta_v' w'}$ is evaluated using the sonic temperature (θ_v) recorded by the ultrasonic anemometers, and the Monin-Obukhov length scale (L) and the stability parameter (z/L) are subsequently evaluated using Eq. (4). Once the stability parameter (z/L) is obtained, the non-dimensional gradient function (ϕ_m) and the stability function (ψ_m) are readily calculated from Eqs. (7)–(10). These are further used in Eq. (13) in order to evaluate the equivalent wind drag coefficient under neutral stability conditions (C_{DNz}). Lastly, Eq. (14) is used to convert C_{DNz} that is referenced to the anemometer elevation into C_{DN10} which is referenced to $z = 10$ m. The aerodynamic roughness (z_o) that is required for this purpose can be evaluated from the velocity profile in Eq. (5) or (6). In other words, knowing the shear velocity (u_*) and the measured wind speed ($\bar{u}_z$), the velocity profile is solved for the aerodynamic roughness.

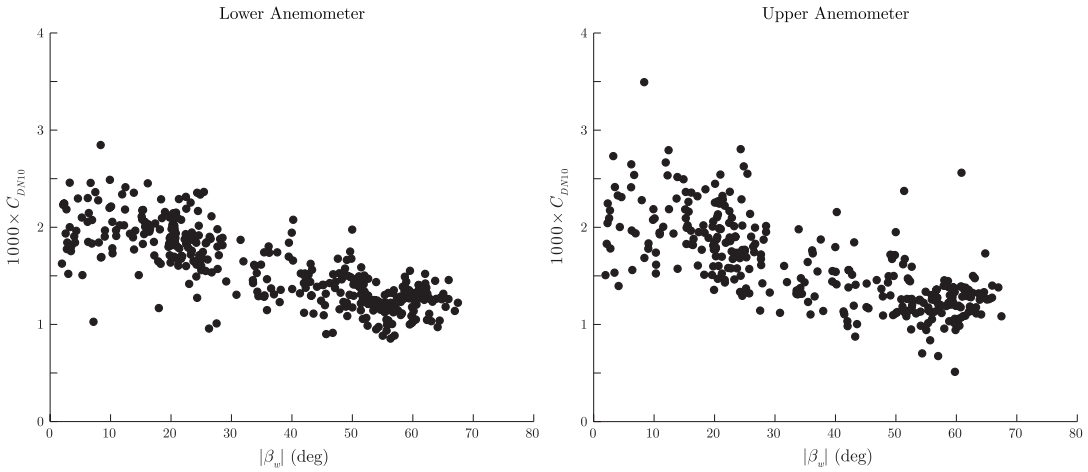

Figure 2: Neutral drag coefficient (C_{DN10}) from the lower (5 m) and upper (10 m) anemometer data versus the angle (β_w) between the wind direction and the shore-normal orientation. Each data point corresponds to a 15-min data run.

RESULTS AND DISCUSSION

A total of 1802 quality-controlled data runs (898 from the lower and 904 from the upper anemometer) each with the duration of 15 minutes were obtained from the eddy correlation measurements of the North Stradbroke 2012 experiment. This amounts to 450 hours of quality-controlled wind data, which includes data collected during different stability conditions. In this paper, only the near-neutral subset of the data, i.e. those with the stability length-scale of $|L| \geq 100$ m, will be discussed.

Directional Distribution of Wind Drag Coefficient

The neutral drag coefficients (C_{DN10}) obtained from the lower (5 m) and upper (10 m) anemometers are plotted in Figures 2a and 2b, respectively. The horizontal axis shows $|\beta_w|$, where β_w is the angle between the "wind direction" and the "cross-shore orientation". Here, $\beta_w = 0$ implies that the wind is blowing onshore and is perpendicular to the shoreline, whereas $\beta_w = \pm 90^\circ$ corresponds to when the wind is in the longshore direction. A key aspect of Figure 2 is that the drag coefficient reduces as β_w increases. In other words, onshore winds blowing perpendicular to the shoreline ($\beta_w = 0$) are characterised by the largest drag coefficients. C_{DN10} systematically drops down as the wind direction changes toward the longshore direction $|\beta_w| = 90^\circ$. The wind direction at this field site often involves a southerly component. Therefore, positive β_w values are more frequently observed. Having said that, it may still be noted that the behaviour of the drag coefficient versus the wind direction was found to be symmetric. That is, negative and positive β_w values are found to exhibit similar drag coefficients. Therefore, the absolute value $|\beta_w|$ has been used in the plots that are shown here.

This behaviour may be explained through the concept of an *apparent wave steepness*. The water waves act as roughness elements for the overhead wind flow. As such, the drag coefficient can be expected to be associated with the wave steepness (H/λ), where H is the wave height and λ is the wave length. The wave steepness has been previously used in the parameterisation of the drag coefficient and roughness in the open ocean (e.g. Taylor and Yelland, 2001). The drag coefficient (C_{DN10}) is expected to increase as waves become steeper. Now, if the wind blows with an angle relative to water waves, the wind will experience longer wave lengths as it travels from one wave crest to another when compared with the condition of wind and waves being completely aligned. The idea of an apparent wave length or subsequently an apparent wave steepness may be defined on this basis. Accordingly, as the wind changes direction from the onshore to the longshore direction, it experiences a smaller apparent wave steepness. The drag coefficient therefore reduces during longshore winds due to this reduced apparent wave steepness.

Figure 3 shows the variations of C_{DN10} with respect to $|\beta_w|$ using $|\beta_w|$ binning intervals of 10°. An empirical relationship explaining the behaviour of C_{DN10} versus β_w may be found by fitting a curve to the data shown in Figure 3. Such an empirical model should include three elements: "onshore C_{DN10}", "longshore C_{DN10}", and "a function of $|\beta_w|$". This function should model C_{DN10} so that it asymptotically reaches its limiting values at the onshore and longshore β_w limits, as can also be concluded from Figure 3. In the present study, onshore winds which produce the largest drag coefficient and therefore the strongest wind forcing on the water surface are of primary interest. Nevertheless, wind with longshore

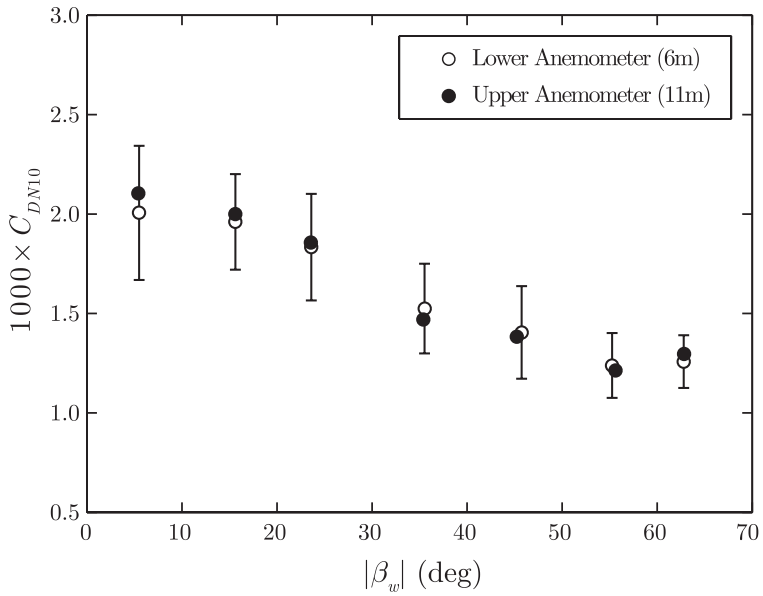

Figure 3: Variations of bin-averaged C_{DN10} with the angle β_w between the wind direction and the shore-normal orientation. The error bars represent the standard deviation for each data bin.

components are also important as they also contribute to storm surge as well as the generation of wind-driven longshore currents. The latter, in combination with the Coriolis force, also generates a rise in water level along the coast for specific wind directions.

Comparison with the Existing Ocean Data

A subset of data which is of the greatest interest in the present study is the near-neutral *onshore* wind data – i.e. those with $0 \leq |\beta_w| < 22.5$. In total, there are 244 such data points, and they will be used here to determine how the wind stress on the surf zone compares with that previously measured in other regions, in particular the open ocean. A common form of parameterisation is to formulate the wind drag coefficient (C_{DN10}) as a linear function of the mean wind speed ($\bar{u}_{N10}$). Here, a set of 12 widely-cited linear drag coefficient formulations are used to compare with results of the present study. These parameterisations are plotted alongside the near-neutral onshore wind data from the present dataset in Figure 4. The results of some major field campaigns such as MARSEN, HEXMAX, WAVES, SWADE, RASEX, ASGAMAGE, and others are represented by the parameterisations plotted here, including measurements in deep water, as well as data collected in shallower regions (depths of 30, 18, 15, 12, or 4 m), but all outside the surf zone. The drag coefficients from the present dataset clearly sit well above other datasets shown here. In fact, the data (∘) yield an average drag coefficient of $C_{DN10} = 2 \times 10^{-3}$. On average and for the same wind speed, the data are characterised by drag coefficients approximately twice those over the ocean. It should also be noted that the amount of scatter in the present data is similar to other air-sea investigations. In fact, a closer look to these data points revealed to the authors that bulk of the scatter is due to run-to-run variations of drag coefficients, rather than systematic changes.

Another widely-used type of parameterisation is to express a normalised form of the sea surface roughness as a function of the wave age parameter (c_p/u_*). The aerodynamic roughness ($z_\circ$) may be normalised in different ways for this purpose. The Charnock coefficient ($\alpha = g z_\circ / {u_*}^2$) is a widely-used normalised roughness. The Charnock coefficient is thought to decrease as the wave-age increases. In other words, actively-growing young seas display larger Charnock's coefficients than fully-developed seas. The functional form of this wave-age dependency is often considered as:

$$\frac{g z_\circ}{{u_*}^2} = a \left(\frac{c_p}{u_*} \right)^{-b} \tag{15}$$

where c_p is the peak wave celerity. The solid curves in Figure 5 represent Eq. (15) using the empirical coefficients a and b suggested by seven previous studies in the literature. These investigations collectively contain measurements over a wide range of water depths from deep water to as shallow as 4 m. On the same graph, the onshore and near-neutral subset of the Stradbroke 2012 data from both anemometers is shown by open circles (∘). The wave-age ($c_{p\circ}/u_*$) values that are used here to plot the data are from wave measurements by the Brisbane Buoy located offshore the field site at the

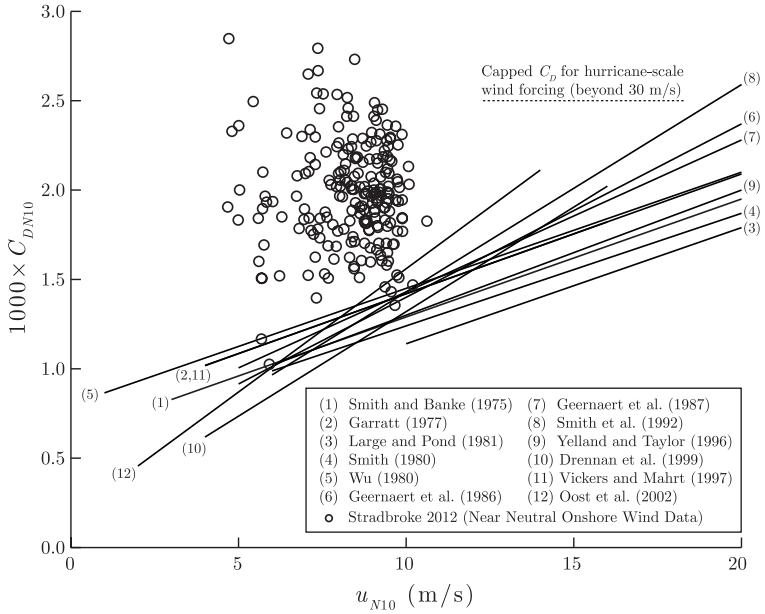

Figure 4: Comparison between neutral drag coefficients (C_{DN10}) measured over the surf zone during the Stradbroke 2012 campaign and those previously reported by other major investigations in other regions of the oceans. Near-neutral onshore wind data from both anemometers are shown for this purpose. Results of previous investigations are based on their proposed linear parameterisation of the drag coefficient versus the wind speed.

depth of 76 m. Note that the use of offshore wave celerity (c_{po}) data is not to imply that measured roughness values are governed by the offshore wave conditions. Instead, offshore wave data are used here to provide an estimate of the aerodynamic roughness offshore from the field site in deeper waters when seen in conjunction with the solid lines in Figure 5. Note that the Charnock coefficient values that are typically cited in the literature are between $\alpha = 0.010$ and 0.020. This indeed belongs to fully-developed seas ($25 < c_p/u_* < 30$) as can be deduced from Figure 5. The Charnock coefficients from the Stradbroke 2012 field data sit markedly above previous investigations shown by the solid lines. The average Charnock coefficient for these data is shown by a dotted line, and is approximately 0.110. This is clearly an order of magnitude (or even more) larger than open ocean estimates.

From another perspective, wave-age (c_p/u_*) values in the range of 0 to 10 are required to explain the large roughness values observed in the present study. In fact, $c_p/u_* = 6$ appears to be a good average estimate for this purpose. Arrows in Figure 5 show this concept, requiring the open circles ($\circ$) to be shifted to the left towards much smaller wave-age values in order to become explainable by the existing parameterisations. Shear velocities (u_*) in the subset of the Stradbroke 2012 data used here are mostly between 0.30 and 0.45 m/s, with an average value of $u_* = 0.37$ m/s. A celerity of $c_p = 2.2$ m/s is then needed to provide the required wave-age of $c_p/u_* = 6$. According to shallow water wave theory $c = \sqrt{gh}$, such a small celerity corresponds to a water depth of merely $h = 0.5$ m. Perhaps, the most conservative estimate of h would be achieved by repeating the same approach as above while using the upper limits of u_* and c_p/u_*, namely 0.45 m/s and 10, instead of their average estimates. This leads to $c_p = 4.5$ m/s and $h = 2$ m. This range of water depths corresponds to the inner surf zone. Consequently, wave celerity values of the order of those found in the inner surf zone are required in order to mathematically explain the observed large roughness values using existing parameterisations. However, the present argument is not in any way intended to conclude that the physics of air-sea interaction over the surf zone is the same as that over open oceans. Among other physical contexts, the wave-age has been seen in previous investigations in the context of the relative velocity between wind and waves in order to take the roughness mobility into account. In that sense, c_p/u_* can be used to explain large roughness values encountered over the surf zone. Though, it is now more appropriate to refer to c_p/u_* as "*the wave celerity over the wind shear velocity*" given that the term "*wave age*" is of little relevance in the context of the surf zone. Open ocean waves propagate with much faster speeds than those found in shallow waters. Indeed, for mature seas, wind and waves travel with very close speeds to each other. This has been seen as a reason for the small roughness values observed in open oceans. Hence, a wave celerity of the order of those found in the inner surf zone can explain

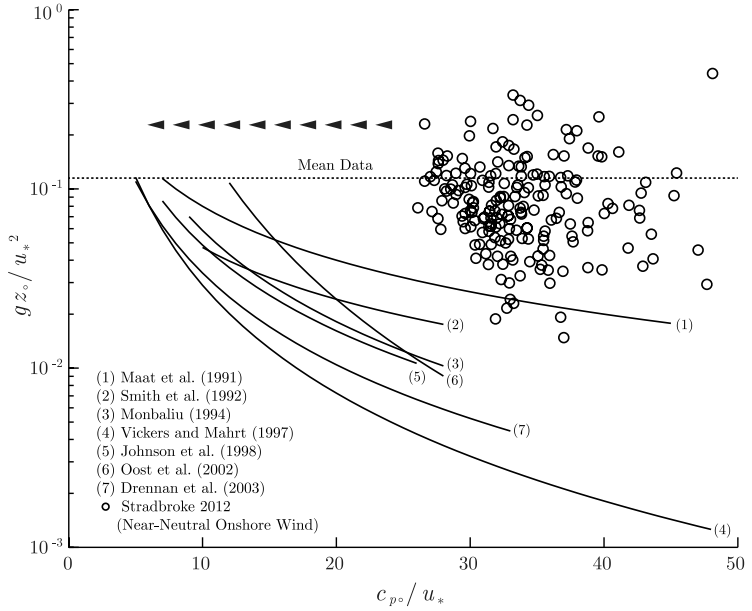

Figure 5: Comparison between the normalised aerodynamic roughness ($gz_\circ/{u_*}^2$) or the Charnock coefficient measured over the surf zone during Stradbroke 2012 campaign and those previously reported by other major investigations in other regions of the oceans. Near-neutral onshore wind data from both anemometers are shown for this purpose. The wave age parameter ($c_{p\circ}/u_*$) that is used here to plot the open circles ($\circ$) is based on the deep water wave celerity. This is evaluated using wave measurements by the Brisbane Buoy at the depth of approximately 76 m offshore the field site at North Stradbroke Island.

the roughness values measured during the Stradbroke 2012 field campaign. However, this is only one difference between surf zone and deep ocean waves. Surf zone waves are of sawtooth shape, compared with deep water waves which have a more sinusoidal shape. One can intuitively expect sawtooth waves in the surf zone to be rougher than more sinusoidal deep water waves, because of flow separation over backward facing step. As such, the wind shear stress is expected to be larger over breaking waves in the surf zone. Slowly travelling waves together with sawtooth wave shapes thus explain the large drag coefficients and roughness values measured over the surf zone.

CONCLUSIONS

An extensive field campaign has been performed to study the wind stress over the surf zone. The eddy correlation technique was adopted for this purpose, with wind data collected using two ultrasonic high-frequency anemometers mounted at nominal heights of 5 and 10 m above the base of a wind mast located in the intertidal and surf zones. The wind drag coefficient was found to systematically change with the wind angle of approach relative to the shoreline. The drag coefficients during longshore winds were on average $C_{DN10} = 1.25 \times 10^{-3}$ and were found to be much smaller than those during onshore winds ($C_{DN10} = 2 \times 10^{-3}$). The differences were explained based on the idea of the apparent wave steepness. The onshore near-neutral subset of the data was compared with the existing studies on the wind drag coefficient and the roughness outside the surf zone. The drag coefficients over the surf zone measured during the Stradbroke 2012 study were found to be on average $C_{DN10} = 2 \times 10^{-3}$ for $\bar{u}_{10} = 5 - 11$ m/s. This is almost twice the values predicted for the same wind speed by existing linear drag coefficient formulations based on observations outside the surf zone. The differences are attributed to different wave celerity and wave shapes in the nearshore region. The observed Charnock coefficient was on average 0.110 which is an order of magnitude larger than open ocean values. The results were also compared with the existing wave-age dependent parameterisations of the Charnock coefficient. It was found that a wave celerity of the order of those observed in the inner surf zone is required to explain the observed large roughness and drag coefficients in the present study using existing wave-age dependent parameterisations.

ACKNOWLEDGEMENTS

This study was sponsored by the ARC Discovery grant DP0877235 provided by the *Australian Research Council*. The authors would like to acknowledge the support of the *Australian Bureau of Meteorology* (BoM) for supplying AWS observations, the *Australian Department of Science, Information Technology, Innovation and the Arts* (DSITIA) for providing Brisbane wave buoy observations, *Maritime Safety Queensland* (MSQ) for supplying Mooloolaba tidal recordings, and *Geoscience Australia* for supplying GIS mapping data.

References

J. A. Businger, J. C. Wyngaard, Y. Izumi, and E. F. Bradley. Flux-profile relationships in the atmospheric surface layer. *Journal of the Atmospheric Sciences*, 28(2):181–189, 1971. ISSN 0022-4928. doi: 10.1175/1520-0469(1971)028<0181:fprita>2.0.co;2. URL http://dx.doi.org/10.1175/1520-0469(1971)028<0181:fprita>2.0.co;2.

H. Charnock. Wind stress on a water surface. *Quarterly Journal of the Royal Meteorological Society*, 81(350):639–640, 1955. doi: 10.1002/qj.49708135027. URL http://dx.doi.org/10.1002/qj.49708135027.

W. M. Drennan, K. K. Kahma, and M. A. Donelan. On momentum flux and velocity spectra over waves. *Boundary-Layer Meteorology*, 92(3):489–515, 1999. ISSN 0006-8314. doi: 10.1023/a:1002054820455. URL http://dx.doi.org/10.1023/a:1002054820455.

W. M. Drennan, H. Graber, D. Hauser, and C. Quentin. On the wave age dependence of wind stress over pure wind seas. *Journal of Geophysical Research*, 108(C3):8062, 2003. doi: 10.1029/2000JC000715. URL http://dx.doi.org/10.1029/2000JC000715.

J. R. Garratt. Review of drag coefficients over oceans and continents. *Monthly Weather Review*, 105 (7):915–929, 1977. ISSN 0027-0644. doi: 10.1175/1520-0493(1977)105<0915:rodcoo>2.0.co;2. URL http://dx.doi.org/10.1175/1520-0493(1977)105<0915:rodcoo>2.0.co;2.

G. L. Geernaert, K. B. Katsaros, and K. Richter. Variation of the drag coefficient and its dependence on sea state. *Journal of Geophysical Research*, 91(C6):7667–7679, 1986. doi: 10.1029/JC091iC06p07667. URL http://dx.doi.org/10.1029/JC091iC06p07667.

G. L. Geernaert, S. E. Larsen, and F. Hansen. Measurements of the wind stress, heat flux, and turbulence intensity during storm conditions over the north sea. *Journal of Geophysical Research*, 92(C12):13127–13139, 1987. doi: 10.1029/JC092iC12p13127. URL http://dx.doi.org/10.1029/JC092iC12p13127.

P. A. Hwang. Influence of wavelength on the parameterization of drag coefficient and surface roughness. *Journal of Oceanography*, 60(5):835–841, 2004. ISSN 0916-8370. doi: 10.1007/s10872-004-5776-8. URL http://dx.doi.org/10.1007/s10872-004-5776-8.

H. K. Johnson, J. Hojstrup, H. J. Vested, and S. E. Larsen. On the dependence of sea surface roughness on wind waves. *Journal of Physical Oceanography*, 28(9):1702–1716, 1998. ISSN 0022-3670. doi: 10.1175/1520-0485(1998)028<1702:otdoss>2.0.co;2. URL http://dx.doi.org/10.1175/1520-0485(1998)028<1702:otdoss>2.0.co;2.

S. A. Kitaigorodskii and Y. A. Volkov. On the roughness parameter of the sea surface and the calculation of momentum flux in the near-water layer of the atmosphere. *Izvestiya Atmospheric and Oceanic Physics (English Translation)*, 1(9):566–574, 1965.

S. Lentz, R. T. Guza, S. Elgar, F. Feddersen, and T. H. C. Herbers. Momentum balances on the north carolina inner shelf. *Journal of Geophysical Research*, 104(C8):18205–18226, 1999. ISSN 2156-2202. doi: 10.1029/1999jc900101. URL http://dx.doi.org/10.1029/1999jc900101.

N. Maat, C. Kraan, and W. A. Oost. The roughness of wind waves. *Boundary-Layer Meteorology*, 54 (1):89–103, 1991. ISSN 0006-8314. doi: 10.1007/bf00119414. URL http://dx.doi.org/10.1007/bf00119414.

W. A. Oost, G. J. Komen, C. M. J. Jacobs, and C. Van Oort. New evidence for a relation between wind stress and wave age from measurements during asgamage. *Boundary-Layer Meteorology*, 103(3):409–438, 2002. ISSN 0006-8314. doi: 10.1023/a:1014913624535. URL http://dx.doi.org/10.1023/a:1014913624535.

C. A. Paulson. The mathematical representation of wind speed and temperature profiles in the unstable atmospheric surface layer. *Journal of Applied Meteorology*, 9(6):857–861, 1970. ISSN 0021-8952. doi: 10.1175/1520-0450(1970)009<0857:tmrows>2.0.co;2. URL http://dx.doi.org/10.1175/1520-0450(1970)009<0857:tmrows>2.0.co;2.

A. J. H. M. Reniers, E. B. Thornton, T. P. Stanton, and J. A. Roelvink. Vertical flow structure during sandy duck: observations and modeling. *Coastal Engineering*, 51(3):237–260, 2004. ISSN 0378-3839. doi: 10.1016/j.coastaleng.2004.02.001. URL http://dx.doi.org/10.1016/j.coastaleng.2004.02.001.

B. Shabani. *Nearshore and Surf Zone Wind Stress*. Thesis, University of Queensland, Brisbane, Australia, 9/9/2013 2013. URL http://dx.doi.org/10.14264/uql.2014.138.

B. Shabani, P. Nielsen, and T. E. Baldock. Field observations of wind stress over surf zone. In J. S. Chung, F. Dias, and H. Kawai, editors, *21st International Offshore and Polar Engineering Conference*, volume 3, pages 991–998, Maui, Hawaii, USA, 19-24 June 2011 2011. ISOPE. ISBN 978-1-880653-96-8.

B. Shabani, P. Nielsen, and T. Baldock. Direct measurements of wind stress over the surf zone. *Journal of Geophysical Research Oceans*, 119, 2014. doi: 10.1002/2013JC009585. URL http://dx.doi.org/10.1002/2013JC009585.

S. D. Smith. Wind stress and heat flux over the ocean in gale force winds. *Journal of Physical Oceanography*, 10(5):709–726, 1980. ISSN 0022-3670. doi: 10.1175/1520-0485(1980)010<0709:wsahfo>2.0.co;2. URL http://dx.doi.org/10.1175/1520-0485(1980)010<0709:wsahfo>2.0.co;2.

S. D. Smith, R. J. Anderson, W. A. Oost, C. Kraan, N. Maat, J. DeCosmo, K. B. Katsaros, K. L. Davidson, K. Bumke, L. Hasse, and H. M. Chadwick. Sea surface wind stress and drag coefficients: The hexos results. *Boundary-Layer Meteorology*, 60(1):109–142, 1992. ISSN 0006-8314. doi: 10.1007/bf00122064. URL http://dx.doi.org/10.1007/bf00122064.

P. K. Taylor and M. J. Yelland. The dependence of sea surface roughness on the height and steepness of the waves. *Journal of Physical Oceanography*, 31(2):572–590, 2001. ISSN 0022-3670. doi: 10.1175/1520-0485(2001)031<0572:tdossr>2.0.co;2. URL http://dx.doi.org/10.1175/1520-0485(2001)031<0572:tdossr>2.0.co;2.

D. Vickers and L. Mahrt. Fetch limited drag coefficients. *Boundary-Layer Meteorology*, 85(1):53–79, 1997. ISSN 0006-8314. doi: 10.1023/a:1000472623187. URL http://dx.doi.org/10.1023/a:1000472623187.

D. Vickers and L. Mahrt. Sea-surface roughness lengths in the midlatitude coastal zone. *Quarterly Journal of the Royal Meteorological Society*, 136(649):1089–1093, 2010. ISSN 1477-870X. doi: 10.1002/qj.617. URL http://dx.doi.org/10.1002/qj.617.

J. Wu. Wind-stress coefficients over sea surface near neutral conditions - a revisit. *Journal of Physical Oceanography*, 10(5):727–740, 1980. ISSN 0022-3670. doi: 10.1175/1520-0485(1980)010<0727:wscoss>2.0.co;2. URL http://dx.doi.org/10.1175/1520-0485(1980)010<0727:wscoss>2.0.co;2.

M. J. Yelland and P. K. Taylor. Wind stress measurements from the open ocean. *Journal of Physical Oceanography*, 26(4):541–558, 1996. ISSN 0022-3670. doi: 10.1175/1520-0485(1996)026<0541:wsmfto>2.0.co;2. URL http://dx.doi.org/10.1175/1520-0485(1996)026<0541:wsmfto>2.0.co;2.

B. C. Zachry, D. Z. Letchford, D. Zuo, J. L. Schroeder, and A. B. Kennedy. Surface drag coefficient behavior during hurricane ike. In *11th Americas Conference on Wind Engineering*, San Juan, Puerto Rico, 22-26 June 2009 2009.